Analysis of winglets and sweep on wind turbine blades using a lifting line vortex particle method in complex inflow conditions

Paper

Sessarego, Matias; Ramos García, Néstor; Shen, Wen Zhong

Published in:
Journal of Physics: Conference Series

Link to article, DOI:
10.1088/1742-6596/1037/2/022021

Publication date:
2018

Document Version
Publisher's PDF, also known as Version of record

Analysis of winglets and sweep on wind turbine blades using a lifting line vortex particle method in complex inflow conditions

IOP Conf. Series: Journal of Physics: Conf. Series **1037** (2018) 022021 doi:10.1088/1742-6596/1037/2/022021

Analysis of winglets and sweep on wind turbine blades using a lifting line vortex particle method in complex inflow conditions

Matias Sessarego, Néstor Ramos-García, Wen Zhong Shen

Department of Wind Energy, Technical University of Denmark, Lyngby Campus, 2800 Kgs. Lyngby, Denmark.

E-mail: matse@dtu.dk

Abstract. An in-house aero-elastic vortex code, called MIRAS, is used to investigate the aerodynamic performance of winglets and sweep on horizontal-axis wind turbine (HAWT) blades in simple and complex inflow conditions. Previous studies using vortex codes applied to study winglets and blade sweep on HAWTs have typically not considered complex inflow conditions such as turbulent wind and shear. The reasons may include the absence of modeling capability, the computational cost associated with simulating long turbulent time series, and/or the computational cost associated with resolving the blade tips to a very fine level. A preliminary study is performed here, where the MIRAS code is applied on the NREL 5 MW wind turbine with an arbitrary winglet shape and blade sweep. Results indicate that wind turbine blades with sweep or winglets might be better in performance compared to their straight blade counterparts.

1. Introduction

There are several studies involving the aerodynamic and aero-elastic analysis or design of winglets and sweep for improving the performance of wind turbine blades. Johansen and Sørensen [1] investigated the aerodynamics of winglets using computational fluid dynamics (CFD) in a parametric study. Elfarra et al. [2] combined CFD with an optimization algorithm to design a winglet on the National Renewable Energy Laboratory (NREL) Phase VI blade. Gaunaa [3] investigated the aerodynamic efficiency of wind turbine rotors with winglets using a free wake lifting line code. Braaten and Gopinath [4] described a vortex line method coupled to ADAMS and performed simulations of wind turbines with winglets and blade sweep. Verelst and Larsen [5] performed a parametric study for forward- and backward-sweep using HAWC2 [6]. Larwood [7] modified NREL's FAST code to account for swept blades and performed aero-elastic simulations with turbulent inflow. Ding and Zhang [8] designed the sweep curve of a 2 MW wind turbine blade using multi-objective optimization. Finally, Pavese et al. [9] designed a wind turbine swept blade using an extensive load analysis.

The current study differs from the previous works in that simulations of horizontal-axis wind turbines (HAWTs) with winglets and sweep are performed using a vortex-based code in more complex inflow conditions. The complex inflow conditions investigated include turbulent wind and extreme shear. While there are several works applying vortex-based codes for wind turbine wake analyses including complex inflow conditions [10, 11, 12, 13], the focus of the present work is to perform a preliminary study of the effect of sweep and winglets compared to straight

blades on HAWTs. References [1, 2, 3, 4] used CFD or vortex codes in simple inflow conditions, while references [5, 7, 8, 9] relied on the lower-fidelity blade element momentum (BEM) based approaches for modeling the aerodynamics. The in-house aero-elastic vortex code used here is called MIRAS, i.e. Method for Interactive Rotor Aero-elastic Simulations. Specifically, the lifting line aerodynamic module is used in the presented study cases, which relies on two-dimensional (or 3D-corrected) polar data for lift and drag. Elasticity is not considered due to the absence of winglet modeling capabilities.

The current article is organized into four sections: Introduction, methodology, results and conclusions. The methodology section briefly describes the MIRAS code and the setup of the simulation cases in two subsections: Simulation tool and simulation setup. The results section contains the results from the simulations and is comprised of four subsections: Non-turbulent inflow, non-turbulent inflow with extreme shear, turbulent inflow, and turbulent inflow with extreme shear. Lastly, conclusions are given in the last section.

2. Methodology

The methodology contains two subsections: Simulation tool and simulation setup. In the first subsection, the MIRAS code will be briefly described. The second subsection will describe the setup for the blade shapes and simulation cases.

2.1. Simulation tool

MIRAS is capable of simulating long time series (>10 min real time) in a few hours of computational time depending on the resolution and number of computing resources used. The high computational efficiency of MIRAS is due to its particle mesh and high performance computing parallelization implementations. In the traditional approach found in free-wake vortex codes, the wake is represented by constructing vortex filaments where the trajectory of its end-markers is governed by the Biot-Savart interaction law. In the particle mesh, the wind turbine wake is represented by particles that are interpolated onto a mesh. The vorticity field is then constructed on the mesh and a Poisson equation is solved for the velocity in Fourier space using a Fast Fourier Transform algorithm. Parallelization in MIRAS is based on the message passing interface (MPI) software. Each simulation in this study uses eighty 2.8 GHz processors on a Linux cluster. Further details regarding MIRAS and the particle mesh implementation are found in [14]. Even though a hybrid filament-mesh vortex method is described in [14], the filament part is replaced by particles and a full particle mesh is employed in the current work instead. Stretching and diffusive terms in the vorticity transport equation are computed using finite-differences in the mesh.

Turbulent inflow in MIRAS is simulated by 1) using the Mann model [15, 16] to generate a velocity field (i.e. a turbulence box), 2) transforming the velocity field into a set of vortex particles (i.e. a particle cloud), and 3) releasing gradually the particle cloud in a plane upstream of the wind turbine rotor. The advantage of using a particle cloud is the ability to simulate free turbulence, where the vorticity due to turbulent wind can interact with the vorticity generated by the interaction of the wind with the turbine rotor blades. The methodology represents more accurately the physics occurring on wind turbines operating in turbulent wind than the traditional frozen-/velocity-based approaches typically used in BEM-based codes such as HAWC2 [6] and FAST [17]. The `windsimu` [18] program is used to generate velocity-field boxes according to the Mann model. The inputs to the `windsimu` program used in the current study are summarized in Table 1.

The wind shear in MIRAS is simulated using a prescribed velocity-vorticity boundary layer method [20]. A Lagrangian implementation of the shear terms in the vorticity transport equation with a slip wall boundary condition to model the ground is used. Shear vorticity in vortex stretching and diffusion is computed using finite differences in the mesh, while convective terms

Table 1: Inputs to the `windsimu` program for generating the Mann turbulence boxes used in MIRAS. The turbulence intensity around hub height is approximately 12.6%.

Input	Description
3	Three-dimensional field
3	All three components to be simulated
4096	Number of longitudinal points
128	Number of horizontal points
128	Number of vertical points
6400	Longitudinal length in meters
180	Horizontal length in meters
180	Vertical length in meters
land	Flat, homogeneous land configuration
8	Mean wind speed
90	Height above the surface
0.2	Roughness length
0	Spectrum type
-5	Random Seed

are given by the particle motion. An extreme power-law wind shear coefficient of 0.45 is employed in all wind shear cases presented in the current article. Details on the inflow turbulence and wind shear modeling are described in detail in [19, 20].

2.2. Simulation setup

To investigate the effect of winglets and sweep on wind turbine performance, the NREL 5 MW wind turbine is used as the reference turbine. Polar data from [21], which includes three-dimensional (3D) corrections for rotational effects near the blade root region, is employed in the lifting line procedure. The flow around the tip for blades with winglets can be highly 3D, thus the employment of uncorrected polar data in this region may be a poor approximation. All simulations are carried out with acknowledgment of this limitation. Figures 1 and 2 depict the surface geometries of the NREL 5 MW blades used in the current study. Be aware that the blades in MIRAS are simulated as lifting lines and not as 3D surfaces. Therefore, all 3D surface geometries shown in the current article are for visualization purposes. Figure 1 depicts the blade (a) without and (b) with a downstream winglet. Downstream is defined as shown in Figure 4(a). Although there is the issue of tower clearance, only downstream/downwind winglets are investigated in the current study, since downstream winglets have been reported to be more effective than upstream/upwind winglets [1, 3]. Similarly, only backward-swept blades are studied, since backward-sweep and not forward-sweep have been reported to give performance improvements [5, 9]. Figure 2 depicts the blade with and without backward-sweep. The winglet shape and sweep are chosen arbitrarily. The winglet begins at 97.3% of the blade length with a tip that points 3 m downstream.

The following equation is used to define the sweep [22, 23]:

$$y = d_{\text{tip}} \left(\frac{x - x_{\text{start}}}{L_{\text{blade}} - x_{\text{start}}} \right)^{\gamma} \tag{1}$$

where y is the local distance from the pitch axis to the sweep curve, d_{tip} is the distance from the pitch axis to the sweep curve at the blade tip, x is the local distance along the blade measured from the blade root, x_{start} is the position of the beginning of the blade sweep, L_{blade} is the

length of the blade, and γ is the sweep exponent. In the studies that follow, $d_{\text{tip}} = 5.0\,\text{m}$, $x_{\text{start}} = 0.4L_{\text{blade}}$, and $\gamma = 2.0$. To simplify the input for MIRAS, the rotor center was used as reference instead of the blade root in Equation 1. Therefore, the NREL 5 MW rotor radius, 63.0 m, was used for L_{blade} instead of the blade length, 61.5 m.

(a) (b)

Figure 1: NREL 5 MW wind turbine blade (a) without and (b) with a downstream winglet.

Section 3 investigates four blade shapes: straight, winglet, swept-short, and swept-long. The main difference between the short and long swept blades is the arc length of the blade. The short swept blade has the same arc length as the straight blade but with a slightly smaller rotor radius. The long swept blade has a slightly larger arc length but with the same rotor radius. Due to the extension, swept-long will have a slightly smaller sweep gradient than swept-short. The blade with the winglet has a larger arc length than the straight blade, but with the same rotor radius. Figure 3 depicts the four blade types investigated. Section 3 investigates the performance of the four blade shapes in four different wind inflow scenarios: Non-turbulent inflow, non-turbulent inflow with extreme shear, turbulent inflow, and turbulent inflow with extreme shear. The MIRAS simulations are performed for wind speeds of 8.0 and 11.4 m/s. The rotor rotational speeds for the 8.0 and 11.4 m/s cases are 9.16 and 12.1 RPM, respectively. The wind speeds and rotor rotational speeds are based on the NREL 5 MW turbine operational conditions [21].

For the simulations that follow, a mesh of approximately $L_x \times L_y \times L_z = 6D \times 1.43D \times 1.43D$ is used, where $D = 126\,\text{m}$ is the rotor diameter and L_x, L_y, L_z are the streamwise, horizontal and vertical domain lengths, respectively. A constant spacing of 1 m is used in all three directions resulting in approximately 24 million cells. The blades are divided into 20 blade segments with cosine spacing. A total of 36000 time steps are simulated. An azimuthal step of 1.5 degrees is used, which is equal to a time step of $1.5 \times 1/(6\,\text{RPM})$ seconds.

3. Results

Section 3 contains the MIRAS simulation results and is comprised of four subsections: Non-turbulent inflow, non-turbulent inflow with extreme shear, turbulent inflow, and turbulent inflow with extreme shear.

Figure 2: NREL 5 MW wind turbine blade with (solid) and without (mesh) sweep.

Figure 3: The four blade types investigated: straight (solid gray), winglet (wire-frame black), swept-short (solid red) and swept-long (wire-frame black).

3.1. Non-turbulent inflow

Figure 4 depicts the instantaneous velocity magnitude for the 8.0 m/s non-turbulent wind inflow simulation of the NREL 5 MW wind turbine with (a) downstream winglets and (b) swept-short blades. The MIRAS simulations are purely aerodynamic and for non-turbulent and uniform winds of 8.0 and 11.4 m/s. The rotor rotational speeds for the 8.0 and 11.4 m/s cases are 9.16 and 12.1 RPM, respectively. The time simulated is between 400-600 seconds excluding transients and mean values are extracted. Tables 2 and 3 contain the numerical values of power and thrust coefficients for the straight, winglet and swept blades. To calculate the coefficients, the rotor radius of the straight blade is used for all cases.

With the exception of swept-short for 8.0 m/s, Tables 2 and 3 shows that adding winglets or sweep to blades increases the power output. The thrust also decreases but not for the swept-long blade. The thrust decreases for the winglet blade because the blade tip is angled away from the wind inflow, decreasing the normal load at the tip. At the same time, more power is achieved because the blades are longer, providing more torque. The difference in power and thrust for the short and long swept blades is due to the differences in rotor radius. The short swept blade produces less thrust because the rotor radius is smaller.

Table 2: Power and thrust for the straight, winglet and swept blades. Non-turbulent and uniform wind at 8.0 m/s with a rotor rotational speed of 9.16 RPM.

Quantity	Straight	Winglet	Swept-short	Swept-long
Power coefficient [-]	0.4942	0.5007	0.4939	0.5011
Power diff.	0.0000%	+1.3132%	-0.0583%	+1.4067%
Thrust coefficient [-]	0.8010	0.8008	0.7968	0.8090
Thrust diff.	0.0000%	-0.0253%	-0.5160%	+1.0012%

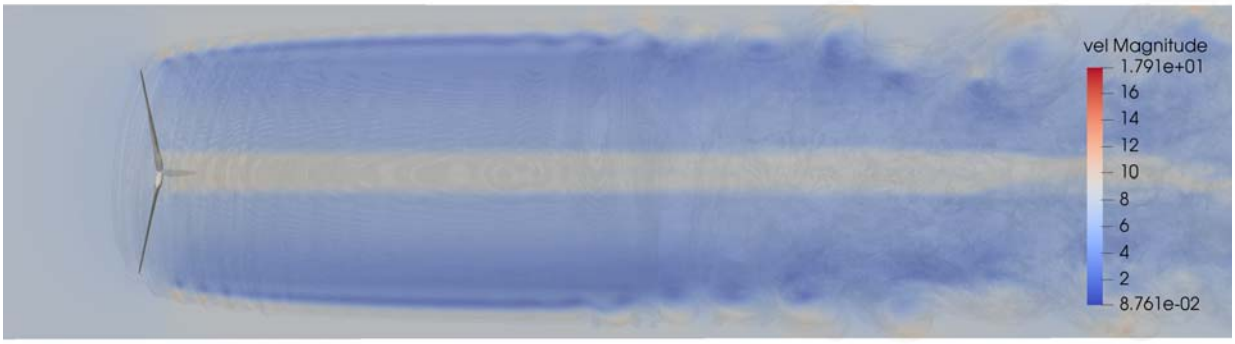

(a)

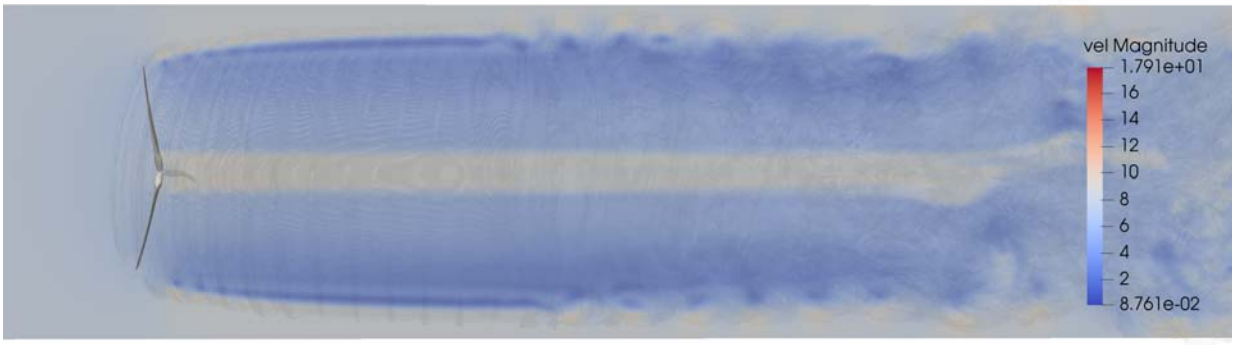

(b)

Figure 4: Instantaneous velocity magnitude for the 8.0 m/s non-turbulent inflow simulation of the NREL 5 MW wind turbine with (a) downstream winglets and (b) swept-short blades. Wind inflow is from left to right.

Table 3: Power and thrust for the straight, winglet and swept blades. Non-turbulent and uniform wind at 11.4 m/s with a rotor rotational speed of 12.1 RPM.

Quantity	Straight	Winglet	Swept-short	Swept-long
Power coefficient [-]	0.4866	0.4912	0.4870	0.4940
Power diff.	0.0000%	+0.9528%	+0.0743%	+1.5234%
Thrust coefficient [-]	0.7576	0.7566	0.7545	0.7657
Thrust diff.	0.0000%	-0.1264%	-0.4044%	+1.0752%

3.2. Non-turbulent inflow with extreme shear

Figure 5 depicts the instantaneous velocity magnitude for the 8.0 m/s non-turbulent wind inflow simulation with extreme shear of the NREL 5 MW wind turbine with (a) straight and (b) winglet blades. The MIRAS simulations are purely aerodynamic with mean wind speeds of 8.0 and 11.4 m/s. There is no controller, therefore the rotor rotational speed is fixed at 9.16 and 12.1 RPM for the 8.0 and 11.4 m/s cases, respectively. The time simulated is between 400-600 seconds excluding transients.

Tables 4 and 5 contain the mean values of torque and thrust, as well as percent differences, for the straight, winglet and swept blades. Tables 4 and 5 are for the non-turbulent 8.0 and 11.4 m/s wind shear cases, respectively. The tables indicate that the winglet and swept-short

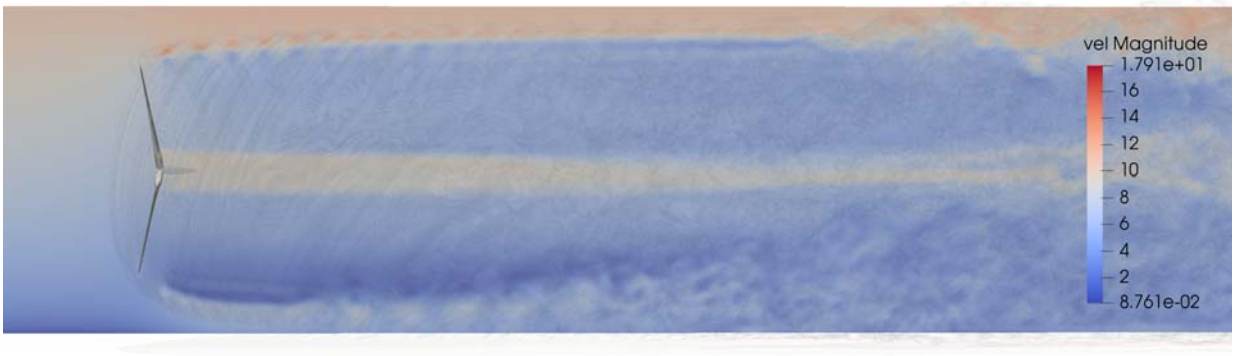

(a)

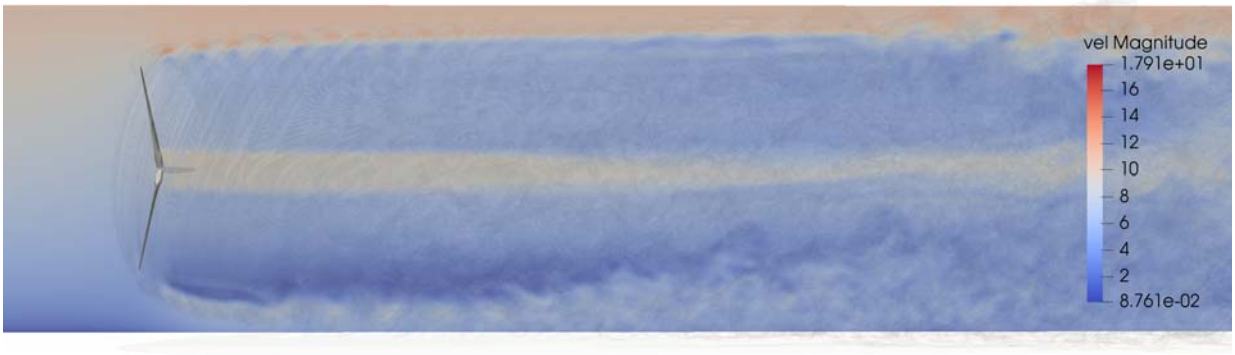

(b)

Figure 5: Instantaneous velocity magnitude for the 8.0 m/s non-turbulent inflow simulation with extreme shear of the NREL 5 MW wind turbine with (a) straight and (b) winglet blades. Wind inflow is from left to right.

blades out-perform the straight blade in terms of torque and thrust for both the 8.0 and 11.4 m/s cases. Similar to the findings in Tables 2 and 3, the winglet blade produces less thrust compared to the straight blade particularly for higher wind speeds.

Table 4: Mean torque and thrust for the straight, winglet and swept blades. Non-turbulent wind at 8.0 m/s with an extreme shear exponent of 0.45 and a rotor rotational speed of 9.16 RPM.

Quantity	Straight	Winglet	Swept-short	Swept-long
Torque mean [N m]	2.083e+06	2.107e+06	2.090e+06	2.120e+06
Torque diff.	0.000%	+1.112%	+0.310%	+1.723%
Thrust mean [N]	3.926e+05	3.923e+05	3.911e+05	3.970e+05
Thrust diff.	0.000%	-0.074%	-0.363%	+1.115%

3.3. Turbulent inflow

Figure 6 depicts the instantaneous velocity magnitude for the simulations of the NREL 5 MW wind turbine with (a) straight and (b) swept-short blades. The MIRAS simulations are purely aerodynamic and for a turbulent wind inflow with a mean wind speed of 8.0 m/s. There is no controller, therefore the rotor rotational speed is fixed at 9.16 RPM. The time simulated is

Table 5: Mean torque and thrust for the straight, winglet and swept blades. Non-turbulent wind at 11.4 m/s with an extreme shear exponent of 0.45 and a rotor rotational speed of 12.1 RPM.

Quantity	Straight	Winglet	Swept-short	Swept-long
Torque mean [N m]	4.441e+06	4.477e+06	4.457e+06	4.518E+06
Torque diff.	0.000%	+0.810%	+0.362%	+1.740%
Thrust mean [N]	7.501e+05	7.489e+05	7.476e+05	7.583e+05
Thrust diff.	0.000%	-0.170%	-0.342%	+1.094%

(a)

(b)

Figure 6: Instantaneous velocity magnitude for the 8.0 m/s turbulent wind inflow simulation of the NREL 5 MW wind turbine with (a) straight and (b) swept-short blades. Wind inflow is from left to right.

approximately 600 seconds excluding transients.

Table 6 contains the numerical values of torque, thrust, and blade 1 flapwise root-bending moment (Mf1) for the straight, winglet and swept blades. The equivalent load (EqL) based on Mf1 is calculated using rainflow counting for a 20-year lifespan ($20\times365\times24\times60\times60$), a frequency of 1 Hz, and a material exponent of $m = 10$. Other quantities include the mean, maximum, minimum, and the standard deviation (STD). The row labeled as "Score" in Table 6 represents the sum of the scoring from all quantities for each column in the table. Each quantity for each blade type is given a score between 1 and 4 based on its performance with respect to the other blade types. For example, swept-long has the highest "Torque mean", thus is assigned 4 points. Straight has the lowest mean torque, thus is assigned only 1 point. Winglet and swept-short are

assigned 3 and 2 points, respectively, based on the sorting of the mean torque. Similarly, the scoring for the mean thrust is: Straight (2 points), winglet (3 points), swept-short (4 points) and swept-long (1 point). The blade type with the highest total score will be the most preferable blade based on this scoring system. A lower STD should lower fatigue loads and is preferred over a higher STD.

Table 6: Torque, thrust, and blade 1 flapwise root-bending moment (Mf1) for the straight, winglet and swept blades. Turbulent inflow with a mean wind speed of 8.0 m/s and a rotor rotational speed of 9.16 RPM. EqL = equivalent load for a 20-year lifespan and STD = standard deviation.

Quantity	Straight	Winglet	Swept-short	Swept-long
Torque mean [N m]	2.062E+06	2.087E+06	2.066E+06	2.097E+06
Thrust mean [N]	3.928E+05	3.926E+05	3.911E+05	3.972E+05
Torque STD [N m]	2.647E+05	2.650E+05	2.680E+05	2.691E+05
Thrust STD [N]	2.287E+04	2.275E+04	2.307E+04	2.314E+04
Torque max [N m]	3.100E+06	3.124E+06	3.112E+06	3.149E+06
Thrust max [N]	4.720E+05	4.711E+05	4.705E+05	4.769E+05
Torque min [N m]	1.428E+06	1.452E+06	1.432E+06	1.453E+06
Thrust min [N]	3.328E+05	3.337E+05	3.320E+05	3.378E+05
Mf1 EqL [N m]	1.940E+06	1.908E+06	1.943E+06	1.966E+06
Mf1 mean [N m]	5.611E+06	5.592E+06	5.574E+06	5.695E+06
Mf1 max [N m]	7.634E+06	7.582E+06	7.594E+06	7.741E+06
Mf1 min [N m]	3.898E+06	3.910E+06	3.876E+06	3.962E+06
Mf1 STD [N m]	4.823E+05	4.777E+05	4.851E+05	4.914E+05
Score	30	41	37	22

The scoring system used implies that the winglet blade, with 41 points, is the most preferred blade type out-of the four blades. The least preferred blade type is the swept-long blade with only 22 points. Swept-long performs poorly because it received 1 point for all quantities except for Torque mean, Torque max, and Torque min. Although the results suggest that winglet and swept-short may perform better in turbulent wind than the straight blade, the results shown in Table 6 are influenced by the resolution of the mesh. Furthermore, they are based on a single wind speed and turbulence seed. More simulations with different wind speeds and turbulence seeds including aero-elastic effects and a controller should be performed to check if similar results are obtained. In addition, the differences in geometry between swept-short and swept-long are quite small and both produce a very different score. Changing the winglet or sweep dimensions slightly may change the results significantly.

3.4. Turbulent inflow with extreme shear

Figure 7 depicts the instantaneous velocity magnitude for the 8.0 m/s turbulent inflow simulation with extreme shear of the NREL 5 MW wind turbine with (a) straight and (b) swept-long blades. The MIRAS simulations are purely aerodynamic and for a mean wind speed of 8.0 m/s. There is no controller, therefore the rotor rotational speed is fixed at 9.16 RPM. The time simulated is approximately 600 seconds excluding transients.

Table 7 contains the numerical values of torque, thrust, and Mf1 for the straight, winglet and swept blades. All quantities, i.e. mean, max, min, STD, EqL, etc., and the meaning of the "Score" row are the same as described in subsection 3.3. The scoring system used in Table 7 implies that the swept-short blade, with 43 points, is the most preferred blade type out-of the

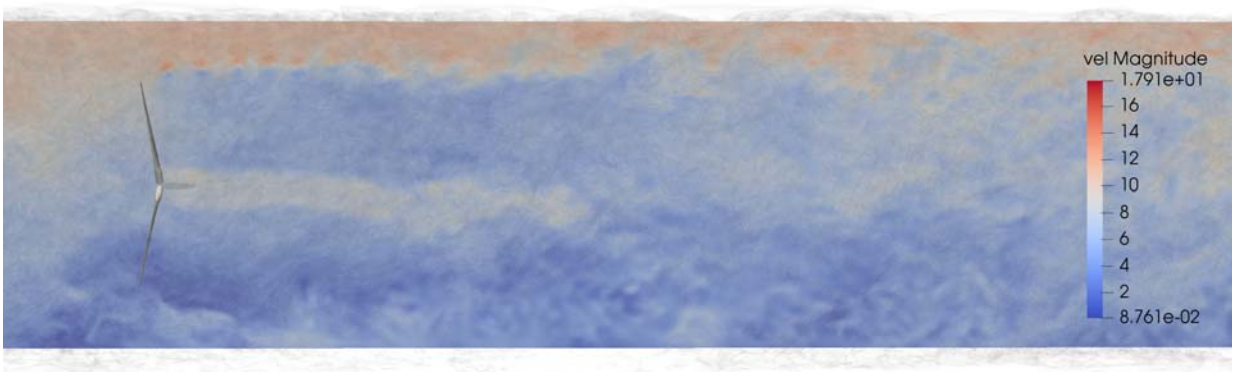

(a)

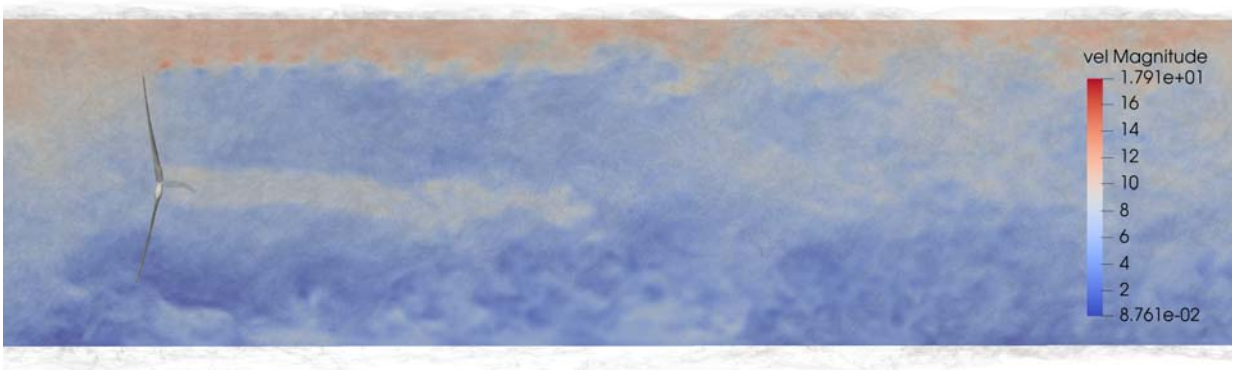

(b)

Figure 7: Instantaneous velocity magnitude for the 8.0 m/s turbulent inflow simulation with extreme shear of the NREL 5 MW wind turbine with (a) straight and (b) swept-long blades. Wind inflow is from left to right.

four blades. The least preferred blade type is the swept-long blade with only 21 points due to high thrust and Mf1 values. The results in Table 7 are similar to those in Table 6, except the winglet blade came second instead of first for the highest score. Swept-short scored better than winglet because of lower STD, thrust, and Mf1 values. More simulations with finer blade and mesh grids may be required to quantify statistically which blade type performs better than the other types.

4. Conclusions

An in-house aero-elastic vortex code, called MIRAS, is used to investigate the aerodynamic performance of winglets and sweep on wind turbine blades in simple and complex inflow conditions. Previous studies using vortex codes applied to study winglets and blade sweep have typically not considered complex inflow conditions such as turbulent wind and shear. While there are several works applying vortex-based codes for wind turbine wake analyses including complex inflow conditions, the focus of the present work was to perform a preliminary study of the effect of sweep and winglets compared to straight blades on horizontal-axis wind turbines (HAWTs). The MIRAS code is applied on the NREL 5 MW wind turbine with an arbitrary winglet shape and blade sweep. Results for simpler inflow conditions indicate that HAWT blades with sweep or winglets may be better in performance compared to their straight blade counterparts. For complex inflow cases such as turbulent wind with extreme shear, shorter-swept and winglet blades received the highest score because they produced lower loads on the

Table 7: Torque, thrust, and blade 1 flapwise root-bending moment (Mf1) for the straight, winglet and swept blades. Turbulent inflow with extreme shear, a mean wind speed of 8.0 m/s, and a rotor rotational speed of 9.16 RPM. EqL = equivalent load for a 20-year lifespan and STD = standard deviation.

Quantity	Straight	Winglet	Swept-short	Swept-long
Torque mean [N m]	2.050E+06	2.078E+06	2.061E+06	2.091E+06
Thrust mean [N]	3.846E+05	3.849E+05	3.836E+05	3.893E+05
Torque STD [N m]	3.155E+05	3.175E+05	3.119E+05	3.197E+05
Thrust STD [N]	2.872E+04	2.856E+04	2.824E+04	2.887E+04
Torque max [N m]	3.170E+06	3.221E+06	3.167E+06	3.219E+06
Thrust max [N]	4.720E+05	4.732E+05	4.693E+05	4.767E+05
Torque min [N m]	1.255E+06	1.301E+06	1.266E+06	1.300E+06
Thrust min [N]	3.067E+05	3.093E+05	3.060E+05	3.126E+05
Mf1 EqL [N m]	3.176E+06	3.103E+06	3.127E+06	3.201E+06
Mf1 mean [N m]	5.486E+06	5.476E+06	5.458E+06	5.573E+06
Mf1 max [N m]	7.884E+06	7.834E+06	7.752E+06	7.928E+06
Mf1 min [N m]	2.196E+06	2.318E+06	2.193E+06	2.228E+06
Mf1 STD [N m]	1.074E+06	1.051E+06	1.065E+06	1.092E+06
Score	29	37	43	21

wind turbine. Further studies are required to investigate the effect of blade and mesh resolution, varying dimensions for winglets and sweep, as well as adding more simulations with different wind speeds and turbulence seeds.

References

[1] Johansen J and Sørensen N N 2006 Aerodynamic investigation of winglets on wind turbine blades using CFD Tech. Rep. Risø-R-1543(EN) Risø National Laboratory Roskilde, Denmark
[2] Elfarra M A, Sezer-Uzol N and Akmandor I S 2014 *Wind Energy* **17** 605–626 ISSN 1099-1824 URL http://dx.doi.org/10.1002/we.1593
[3] Gaunaa M and Johansen J 2007 *Journal of Physics: Conference Series* **75** 012006 URL http://stacks.iop.org/1742-6596/75/i=1/a=012006
[4] Braaten M E and Gopinath A 2011 Aero-structural analysis of wind turbine blades with sweep and winglets: Coupling a vortex line method to ADAMS/AeroDyn GT2011-45904 (Proceedings of ASME Turbo Expo 2011)
[5] Verelst D and Larsen T 2010 *Load Consequences when Sweeping Blades - A Case Study of a 5 MW Pitch Controlled Wind Turbine* (Danmarks Tekniske Universitet, Risø Nationallaboratoriet for Bæredygtig Energi)
[6] Larsen T J and Hansen A M 2007 *HAWC2 - User manual* DTU-Risø-R-1597
[7] Larwood S and van Dam C 2013 *Wind Energy* **16** 879–907 ISSN 1099-1824 URL http://dx.doi.org/10.1002/we.1529
[8] Ding Y and Zhang X 2016 *Journal of Renewable and Sustainable Energy* **8** 043303 URL https://doi.org/10.1063/1.4961588
[9] Pavese C, Kim T and Murcia J P 2017 *Renewable Energy* **102** 21 – 34 ISSN 0960-1481 URL http://www.sciencedirect.com/science/article/pii/S0960148116309041
[10] Scheurich F, Fletcher T M and Brown R E *Wind Energy* **14** 159–177 (*Preprint* https://onlinelibrary.wiley.com/doi/pdf/10.1002/we.409) URL https://onlinelibrary.wiley.com/doi/abs/10.1002/we.409
[11] Chatelain P, Backaert S, Winckelmans G and Kern S 2013 *Flow, Turbulence and Combustion* **91** 587–605 ISSN 1573-1987 URL https://doi.org/10.1007/s10494-013-9474-8
[12] Chatelain P, Duponcheel M, Caprace D G, Marichal Y and Winckelmans G 2016 *Journal of Physics: Conference Series* **753** 032007 URL http://stacks.iop.org/1742-6596/753/i=3/a=032007

[13] Chatelain P, Duponcheel M, Zeoli S, Buffin S, Caprace D G, Winckelmans G and Bricteux L 2017 *Journal of Physics: Conference Series* **854** 012011 URL http://stacks.iop.org/1742-6596/854/i=1/a=012011
[14] Ramos-García N, Hejlesen M M, Sørensen J N and Walther J H 2017 *Wind Energy* **20** 1871–1889 ISSN 1099-1824 we.2126 URL http://dx.doi.org/10.1002/we.2126
[15] Mann J 1994 *Journal of Fluid Mechanics* **273** 141–168 ISSN 1469-7645
[16] Mann J 1998 *Probabilistic Engineering Mechanics* **13** 269 – 282 ISSN 0266-8920 URL http://www.sciencedirect.com/science/article/pii/S0266892097000362
[17] Jonkman J M and Buhl M L 2005 *FAST User's Guide* National Renewable Energy Laboratory Golden, Colorado. NREL/EL-500-29798
[18] Mann J *windsimu a program for simulation of turbulence in complex terrain* Technical University of Denmark
[19] Rasmussen J and Walther J 2011 *Particle Methods in Bluff Body Aerodynamics* Ph.D. thesis the Ph.D. Project was funded by the Danish Research Council of Independent Research (Grant. No. 274-08-0258)
[20] Ramos-García N, Spietz H J, Sørensen J N and Walther J H 2018 *Wind Energy* Vortex simulations of wind turbines operating in atmospheric conditions using a prescribed velocity-vorticity boundary layer model. Submitted February 2018
[21] Jonkman J, Butterfield S, Musial W and Scott G 2009 Definition of a 5-MW reference wind turbine for offshore system development Tech. rep.
[22] Zuteck M 2002 Adaptive blade concept assessment: Curved planform induced twist investigation Tech. Rep. SAND2002-2996 Sandia National Laboratories Albuquerque, New Mexico 87185 and Livermore, California 94550
[23] Larwood S, van Dam C and Schow D 2014 *Renewable Energy* **71** 563 – 571 ISSN 0960-1481 URL http://www.sciencedirect.com/science/article/pii/S0960148114003115